International Journal of Fluid Power 3 (2002) No. 1 pp. 7-20

COMPUTER AIDED OPTIMIZATION OF BEARING AND SEALING GAPS IN HYDROSTATIC MACHINES - THE SIMULATION TOOL CASPAR

Uwe Wieczorek and Monika Ivantysynova

Technical University of Hamburg-Harburg, Institute for Aircraft Systems Engineering, Nesspriel 5, 21129 Hamburg, Germany
U.Wieczorek@tu-harburg.de, M.Ivantysynova@tu-harburg.de

Abstract

The simulation tool CASPAR (**Ca**lculation of **s**wash **p**late type **a**xial piston pump and moto**r**) is presented in this paper. Based on the simulation of the flow through the lubricating gaps in swash plate type axial piston machines the pressure, velocity and temperature fields in the considered gaps can be determined. This allows the calculation of the main losses generated in the machine due to viscous friction and gap flow. The individual gaps are connected in a complex way to each other. The calculation of the gap flow requires the determination of the instantaneous gap heights for all considered gaps. This is realized by solving the motion equation for all moveable parts of the rotating group. For determination of pressure dependent external forces the instantaneous pressure in the displacement chamber is calculated simultaneously. The program further calculates the instantaneous inlet and outlet flow of the swash plate machine for pumping and motoring mode as well as internal volumetric losses.

Keywords: axial piston machine, non-isothermal gap flow, prediction of losses, computer aided design of swash plate machines

This manuscript was received on 31 January 2002 and was accepted after revision for publication on 21 March 2002

1 Introduction

The enormous increase in the performance of computer hardware makes the use of computer aided engineering tools possible for many applications in almost all branches of engineering. Since the development of hydrostatic machines is usually based on experience made with former products and many tests are necessary, it is desirable that computer aided engineering tools can be used for the design of hydrostatic machines. At the Institute for Aircraft Systems Engineering of the Technical University of Hamburg-Harburg the simulation tool CASPAR (Calculation of Swash Plate Type Axial Piston Pump/Motor) has been developed. The developed simulation tool is focused on swash plate type axial piston machines. For the design of displacement machines the computation of gap flow plays an important role. The gaps in displacement machines undertake usually two different functions. The gap serves as sliding bearing between the parts, moving relatively to each other and accomplishes a sealing function. Due to this double function the gap geometry is not a constant value but depends on the particular operation parameters of the displacement machine, mainly on the operating pressure, the rated speed, the viscosity of the fluid and in case of variable displacement units also on the adjusted displacement volume. The gap geometry influences strongly the volumetric and friction losses of the displacement machine and with it the achievable efficiency. For the development of hydrostatic pumps and motors with higher efficiency rates and with a simultaneously high service life an optimal gap design allowing a minimum of friction and volumetric losses in the given parameter range of the machine is urgently necessary. There has been a series of reasons which had not allowed the application of appropriate design methods in the past. For example the gap geometry leads mostly to mathematical models with partial differential equations describing the laminar gap flow, which can be solved only numerically, i.e. an appropriate computer performance is needed. Further the gaps in displacement machines are self-adjusting, i.e. the instantaneous gap geometry is given by the equilibrium of forces acting on the individual parts resulting from the operating parameters of the machine. This requires a simultaneous gap simulation of all concerned gaps, whereas the individual gap heights are calculated for each time step with the help of the mo-

tion equation of all moveable parts of the rotating group .

Besides these an energy dissipation occurs due to the flow of a viscous fluid in the gap. The fluid and the whole displacement unit is heated up by the dissipated energy. The increase of temperature of the fluid and with it the decrease of viscosity leads to a higher volumetric flow through the gap and a lower load capacity of the gap. Both influences cannot be neglected, i.e. the gap flow simulation model must consider the non-isothermal flow conditions. Therefore the energy equation, as a second partial differential equation has to be solved within the program.

For the first time it is possible to calculate the gap flow and thus the losses due to viscous friction and leakage in all gaps of the rotating group of a swash plate machine with the here presented simulation tool CASPAR.

2 Simulation Tool

The calculation of the gap flow in the sealing and bearing gaps of a swash plate machine is based on a mathematical model of the non-isothermal gap flow as explained in chapter 3. The simulation of the non-isothermal gap flow is applied for the gaps between piston and cylinder, between slipper and swash plate and between cylinder block and valve plate, as shown in Fig. 1. To determine the gap flow the gap height is calculated by solving the motion equation for all moving parts, as explained in chapter 5. The balance of fluid forces in the gaps and external forces are considered in the motion equation. Since the pressure in the displacement chamber determines the pressure dependent external forces the calculation of the instantaneous pressure in the displacement chamber is also included in the simulation program, see chapter 4. The simulation is done simultaneously for all gaps, to take the influence between each gap into account. In order to verify the simulation model various measurements have been done, e.g. measurement of the instantaneous pressure in the displacement chamber (Wieczorek and Ivantysynova, 2000), friction force measurements (Ivantysynova, 1999; Lasaar and Ivantysynova, 2001) and steady state measurements (Wieczorek, 2000).

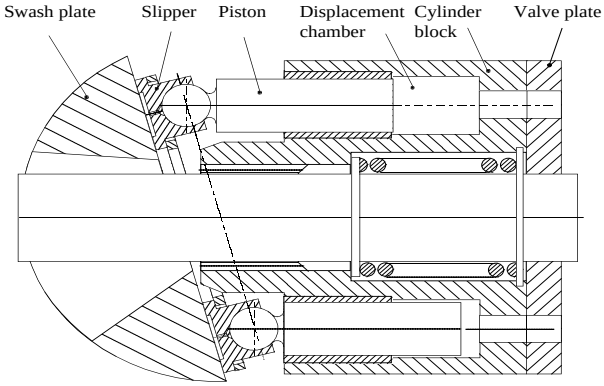

Fig. 1: *Swash plate type axial piston pump*

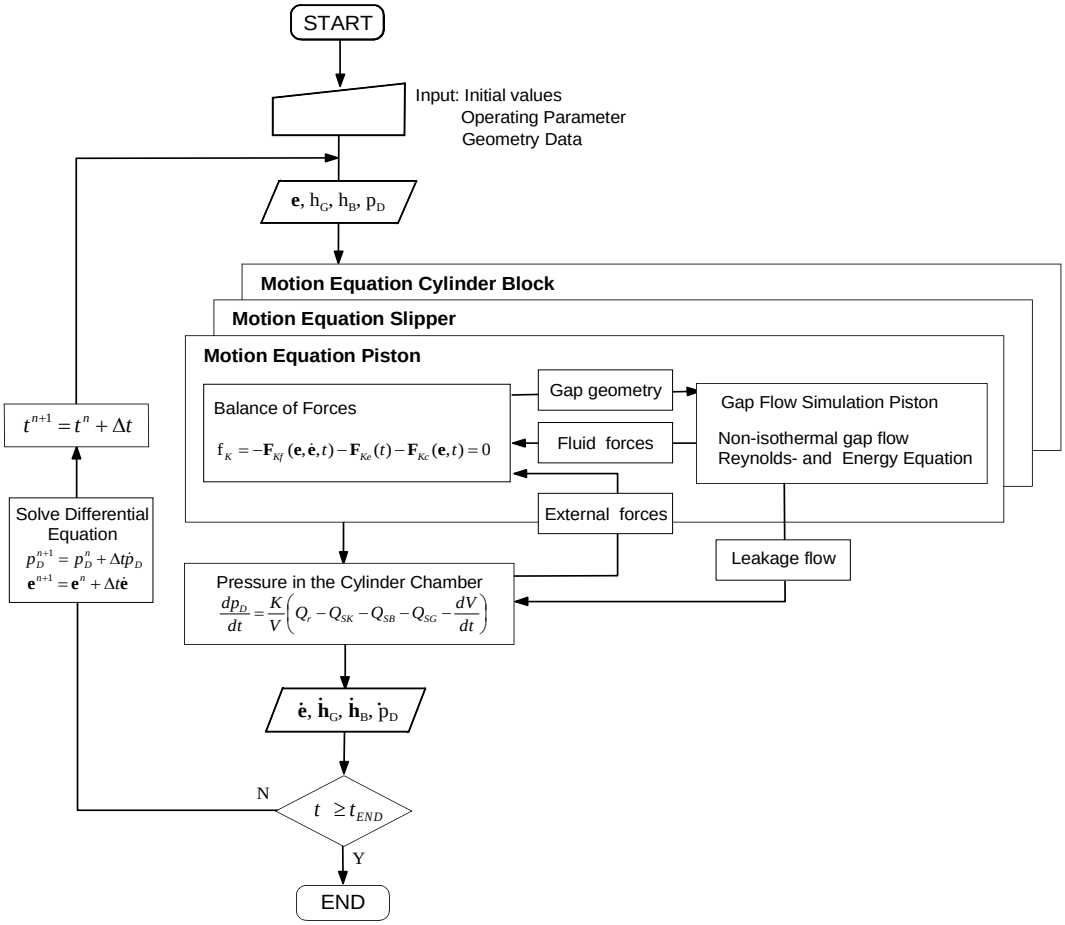

Fig. 2: *Structure of the Simulation Tool CASPAR*

Figure 2 shows the principal structure of the simulation program. The operating parameter, the design parameters and the initial values are the inputs of the program. The motion equation is solved sequentially for each component. Since the gap geometry determines the hydrodynamic pressure field in the gap, iteration has to be done to solve the motion equation. Hence the pressure and temperature field and the velocity distribution in the gap have to be calculated several times in each time step. With the pressure field the fluid force can be calculated and based on the velocity distribution the leakage and viscous friction is calculated. The calculated leakage flows are taken into account to determine the pressure in the displacement chamber.

To describe the behaviour of a hydrostatic machine realistically the simultaneous calculation of all gaps is necessary. To compute the position of the components a numerical integration algorithm is used. MATLAB a software tool for numerical mathematics provides various algorithms. MATLAB was also used as basis for the user interface. The gap flow simulation and the motion equation were realized in programming language C and integrated in a MATLAB environment. An optimization of the gap geometry is possible through variation of the parameters.

In the following chapters the calculation of the gap flow and the motion equation is explained on example of the piston/cylinder assembly. The calculation is carried out similarly for the other gaps. Chapter 5 gives a brief introduction of the simulation model for the pressure in the displacement chamber. Finally chapter 6 shows some simulation results to give an overview of the capability of CASPAR.

3 Calculation of the Gap Flow

The calculation of the gap flow is explained for the example of the gap between piston and cylinder. Since the gap-diameter ratio is very small, the gap can be expanded on the $\hat{x}$ - $\hat{y}$ plane (Fig. 3b), where $\hat{x}$ denotes the gap circumference and $\hat{y}$ denotes the gap length. Hence the transformation of the coordinates is given by:

$$\hat{x} = \phi_K R_K \; ; \; \hat{y} = z_K \; ; \; \hat{z} = h(\phi_K, z_K) \tag{1}$$

Due to the very small gap height laminar flow can be assumed. The calculation of the laminar gap flow is based on the fluid momentum equation (Navier-Stokes Equation) and on the conservation of mass.

$$\frac{\partial \mathrm{v}}{\partial t} + \mathbf{v}\ \mathrm{grad}\ \mathbf{v} = -\mathrm{grad}\left(u_M + \frac{\mathbf{p}}{\rho}\right) + \nu\Delta\mathbf{v} \tag{2}$$

$$\mathrm{div}(\rho\,\mathbf{v}) = \frac{\partial(v_{\hat{x}}\rho)}{\partial\,\hat{\mathrm{x}}} + \frac{\partial(v_{\hat{y}}\rho)}{\partial\,\hat{\mathrm{y}}} + \frac{\partial(v_{\hat{z}}\rho)}{\partial\,\hat{\mathrm{z}}} = 0 \tag{3}$$

Assuming an incompressible fluid[1)] and neglecting the inertia forces and the derivative of fluid velocity in $\hat{x}$ and $\hat{y}$ direction of the gap Eq. 2 can be simplified to

1)This assumption is made only for fluid in the gap, not for the fluid in the displacement chamber

$$\mathrm{grad}\,\mathbf{p} = \mu\Delta\mathbf{v} \tag{4}$$

With the assumption made above the fluid velocity is given by integrating Eq. 4.

$$v_{\hat{x}} = \frac{1}{2\mu}\frac{\partial p}{\partial\,\hat{\mathrm{x}}}(\hat{z}^2 - h\hat{z}) + v_{\mathrm{K}x}\frac{\hat{z}}{h}, \tag{5}$$

$$v_{\hat{y}} = \frac{1}{2\mu}\frac{\partial p}{\partial\,\hat{y}}(\hat{z}^2 - h\hat{z}) + v_{\mathrm{K}y}\frac{\hat{z}}{h}. \tag{6}$$

For the gap flow between piston and cylinder the well-known Reynolds equation, can be derived from Eq. 3 and 4:

$$\begin{aligned}&\frac{\partial}{\partial\hat{x}}\left(\frac{\partial p}{\partial\hat{x}}\frac{h^3}{\mu}\right) + \frac{\partial}{\partial\hat{y}}\left(\frac{\partial p}{\partial\hat{y}}\frac{h^3}{\mu}\right) = \\ &+ 6\left((v_{\mathrm{K}x})\frac{\partial h}{\partial\hat{x}} + (v_{\mathrm{K}y})\frac{\partial h}{\partial\hat{y}} + 2\frac{\partial h}{\partial t}\right)\end{aligned} \tag{7}$$

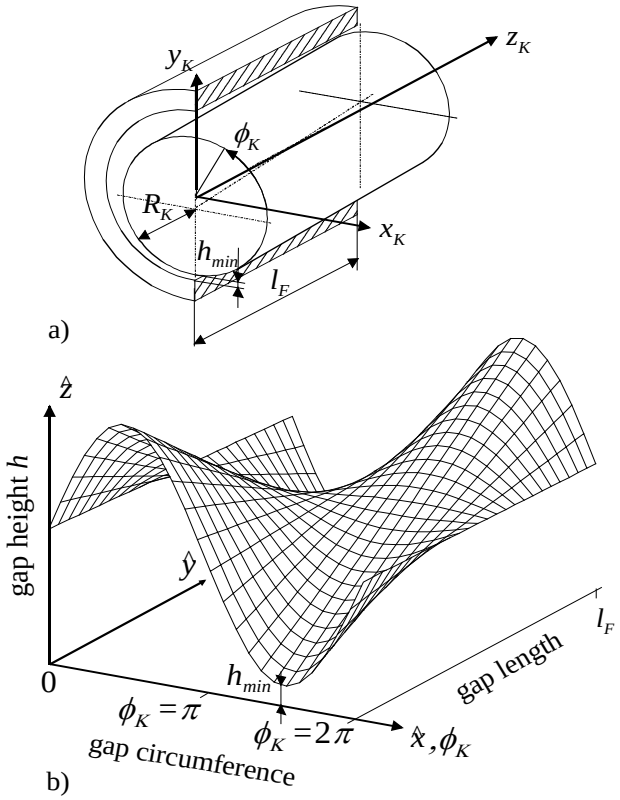

Fig. 3 *Gap between piston and cylinder*

To calculate the gap flow under the slipper and between cylinder block and valve plate the Reynolds equation for cylindrical co-ordinate system is used.

To avoid negative pressure values, a negative value is set to zero when it occurs in the iteration (Krasser and Laback, 1994). Energy dissipation occurs due to friction of the viscous fluid in the gap. The fluid and the whole unit are heated by the dissipated energy. Depending on the thermodynamic state of the liquid, local changes of viscosity can occur. This influence cannot be neglected, thus with decreasing viscosity the flow increase and the load bearing capacity decrease. The

temperature distribution is described by the energy equation:

$$c_p \rho \left(\frac{\partial T}{\partial t} + \mathbf{v}\ \mathrm{grad}\, T \right) = \lambda\, \mathrm{div}\,(\mathrm{grad}\, T) + \mu\ \Phi_D(\mathbf{v}) \qquad (8)$$

The simulation model assumed steady state conditions, thus local changes do not occur $\partial T/\partial t = 0$. For a cartesian system of coordinates the energy dissipation due to fluid friction is given by

$$\Phi_D(\mathbf{v}) = \left(\frac{\partial v_{\hat{x}}}{\partial z} \right)^2 + \left(\frac{\partial v_{\hat{y}}}{\partial z} \right)^2 \qquad (9)$$

with the velocity components v_x and v_y. Once the pressure and temperature distribution is obtained, the change of the viscosity can be evaluated. The pressure and temperature behaviour of the viscosity can be calculated as described in (Ivantysyn, Ivantysynova 2001)

$$\mu = \mu_0 e^{(\alpha_p p - k_T (T - T_0))}. \qquad (10)$$

The pressure distribution is computed based on these results again. The iteration stops if the required precision is achieved. In this manner Reynolds and energy equation are solved simultaneously. Both equations are partial differential equations that can only be solved numerically. Therefore the finite volume method is used (Patankar, 1980). The velocity distribution in the gap can be calculated based on the pressure field. The fluid force is obtained by integrating the pressure field. Equation 11 and 12 give the components of the fluid force in x_K, y_K direction, as shown in Fig. 4

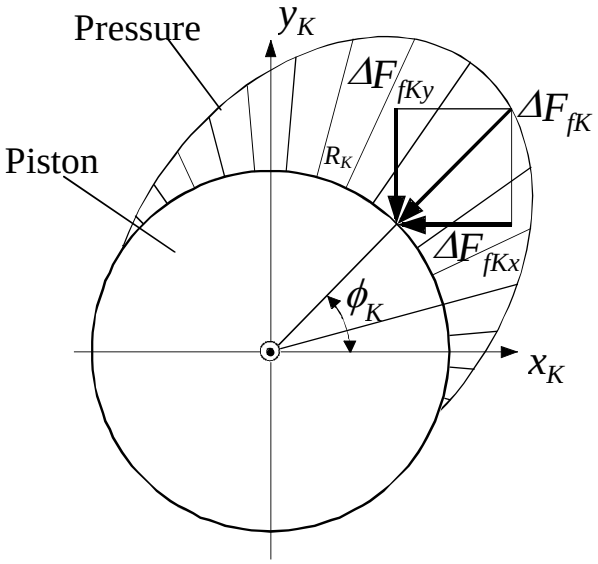

Fig. 4: *Components of the fluid force in the gap between piston and cylinder*

$$F_{fKx} = \int_0^{l_F} \int_0^{2\pi} -p \cos\phi_K R_K d\phi_K d\hat{y} \qquad (11)$$

$$F_{fKy} = \int_0^{l_F} \int_0^{2\pi} -p \sin\varphi_K R_K d\varphi_K d\hat{y} \qquad (12)$$

Equation 13 and 14 are used to calculate the moment exerted on the piston due to the fluid force

$$M_{fKx} = \int_0^{l_F} \int_0^{2\pi} -\hat{y}\ p \sin\phi_K R_K\ d\phi_K d\hat{y}\,, \qquad (13)$$

$$M_{fKy} = \int_0^{l_F} \int_0^{2\pi} \hat{y}\ p \cos\phi_K R_K\ d\phi_K d\hat{y}\,. \qquad (14)$$

Assumed the fluid is a Newtonian Fluid the shearing stress is proportional to the derivation of fluid velocity. Based on the given velocity distribution in the gap shearing stress on the surface τ_{FK} can be calculated. For the viscous friction than follows:

$$F_{TKy}(\varphi) = \int_0^{2\pi R_K} \int_0^{l_F} \tau_{FKy} d\hat{y} d\hat{x} \qquad (15)$$

$$F_{TKx}(\varphi) = \int_0^{2\pi R_K} \int_0^{l_F} \tau_{FKx} d\hat{y} d\hat{x} \qquad (16)$$

The gap flow in direction of the piston axis $\hat{y}$ is obtained by integrating the velocity distribution.

$$Q_{SK_i}(\varphi) = \int_0^{2\pi R_K} \int_0^{h} v_{\hat{y}} d\hat{z} d\hat{x} \qquad (17)$$

4 Pressure in the Displacement Chamber

For the calculation of the gap flow, the instantaneous pressure in the displacement chamber is very important. It defines the boundary conditions for the pressure distribution and determines the pressure dependent external forces exerted on the moveable parts. On the other hand the pressure in the displacement chamber is influenced by the leakage flow in the gaps and the flow through the valve plate, as shown in Fig. 5.

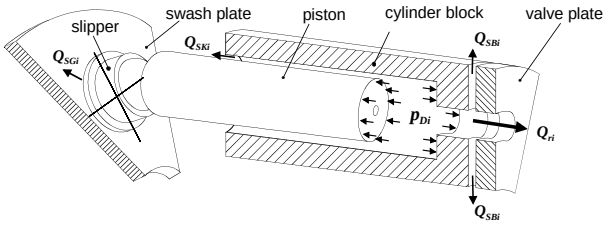

Fig. 5: *Displacement chamber*

The simulation model and the test rig are explained in detail in (Wieczorek and Ivantysynova, 2000). Equation 18 describes the instantaneous pressure p_{Di} in the displacement chamber, where i denote the index of the piston and Q_{ri} denotes the flow through the valve plate.

$$\dot{p}_{Di} = \frac{K}{V_i} \left(Q_{ri} - Q_{SKi} - Q_{SGi} - Q_{SBi} - \frac{dV_i}{dt} \right) \qquad (18)$$

The individual gap flows Q_{SKi}, Q_{SGi} and Q_{SBi} are obtained by the gap flow simulation. The pressure in the suction port and pressure port influences the pressure in the displacement chamber. The pulsation of the flow due to the discrete number of pistons causes pres-

sure pulsation in the high-pressure line by which the bore pressure profile is affected. The calculation of the pressure in the pressure port is also included in the simulation model.

Figure 6 shows the calculated and measured pressure profile for pumping mode. The simulation is based on the following operating parameters:

- 75 cm³ displacement
- 17° swash plate angle
- shaft speed 3000 rpm
- 200 bar pressure difference
- 20 cSt viscosity

For all following calculation results obtained with CASPAR, which are presented in this paper the above mentioned parameters were used. It should be noted that rotating angles between φ = 0° and φ = 180° denote the pump stroke, thus the piston is moving inwards. For rotating angles between φ = 180° and φ = 360° the piston is in suction stroke. The calculation starts at φ = 0°.

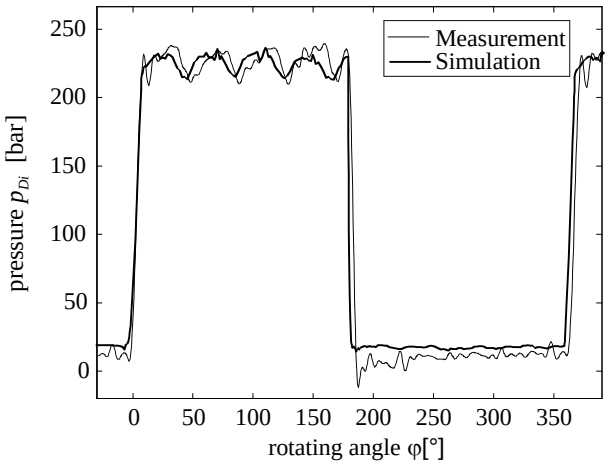

Fig. 6: *Instantaneous pressure in the displacement chamber*

It can be seen that the simulation provides a very good approximation of the pressure profile on the high-pressure side, although a very simple model approximates the flow through the valve plate.

5 Motion Equation

To determine the gap geometry the motion equation for all moving parts is solved. In this chapter the method shall be explained on example of the piston. The motion equation for the cylinder block and slipper carried out similarly and can be found in (Wieczorek and Ivantysynova 2000) and (Wieczorek, 2000).

As shown in Fig. 7, the piston is loaded with a force in an axial direction F_{AKz} due to the inertia force F_{aKz}, friction force F_{TK} and the pressure force F_{DK} :

$$F_{\mathrm{AKz}} = F_{\mathrm{DK}} + F_{\mathrm{aKz}} + F_{\mathrm{TK}} \tag{19}$$

The friction force is calculated based on the shearing stress, Eq. 15 and 16. Since the swash plate in axial piston machines can only balance forces vertically to their surface given by F_{SK}, the piston is loaded with a lateral force $F_{\mathrm{SK}y}$, as shown in Fig. 7. The lateral force $F_{\mathrm{SK}y}$ is given by

$$F_{\mathrm{SK}y} = F_{\mathrm{AKz}} \tan\beta \tag{20}$$

Additionally the piston is loaded with the centrifugal force and with the friction force of the slipper F_{TG}. The centrifugal force is given by

$$F_{\varpi \mathrm{K}} = (m_{\mathrm{K}} + m_{\mathrm{G}})\omega^2 R_{\mathrm{B}} \tag{21}$$

The components of the external force can be expressed as

$$F_{x\mathrm{K}} = -F_{\mathrm{SK}y}\sin\varphi + F_{\mathrm{TG}} \tag{22}$$

$$F_{y\mathrm{K}} = F_{\mathrm{SK}y}\cos\varphi + F_{\omega \mathrm{K}} \tag{23}$$

The moment about x_{K} and y_{K} - axis exerted on the piston due to the external forces is given by

$$M_{x\mathrm{K}} = -z_{\mathrm{RK}}F_{\mathrm{SK}y}\cos\varphi - (z_{\mathrm{RK}} - l_{\mathrm{se}})F_{\omega \mathrm{K}} \tag{24}$$

$$M_{y\mathrm{K}} = z_{\mathrm{RK}}F_{\mathrm{K}x} \tag{25}$$

In case of pumping mode the bushing is loaded with a lateral force to convert the pump input torque into a piston force. The lateral force must be borne by the lubricating film between piston and cylinder.

The position of the piston can be expressed by the eccentricity of the piston $\boldsymbol{e}$ = (e_1,e_2,e_3,e_4) in cross section A and B (Fig. 8).

If the fluid force cannot incorporate the external force, the piston will move in the direction of the external force and due to the 'squeeze' effect, the pressure will increase. The shifting velocity $\dot{\mathbf{e}}$ describes the radial movement of the piston.

In the Reynolds-Equation (Eq. 7) $\partial h/\partial t$ denotes the squeeze film term. This term is calculated by using the shifting velocity, Eq. 26.

$$\begin{aligned}\frac{\partial h(z_{\mathrm{K}},\phi_{\mathrm{K}})}{\partial t} &= -\left(\frac{\dot{e}_3 - \dot{e}_1}{l_{\mathrm{F}}}z_{\mathrm{K}} + \dot{e}_1\right)\cos\phi_{\mathrm{K}} \\ &-\left(\frac{\dot{e}_4 - \dot{e}_2}{l_{\mathrm{F}}}z_{\mathrm{K}} + \dot{e}_2\right)\sin\phi_{\mathrm{K}}\end{aligned} \tag{26}$$

The motion equation is based on the balance of fluid forces, contact forces and external forces that are exerted on the piston (Olems, 2000): For the motion of the piston follows:

$$f_{\mathrm{K}} = -F_{f\mathrm{K}}(e,\dot{e},t) - F_{e\mathrm{K}}(t) - F_{c\mathrm{K}}(e,t) - m_{\mathrm{K}}\ddot{\mathrm{e}} = 0 \tag{27}$$

It should be noted that the inertial force is very small compared to the pressure forces and has been neglected. Thus, with Eq. 28, the motion equation of the piston can be simplified to Eq. 29.

$$F_{f\mathrm{K}} >> m_{\mathrm{K}}\ddot{\mathrm{e}} \tag{28}$$

$$f_{\mathrm{K}} = -F_{\mathrm{f}\mathrm{K}}(e,\dot{e},t) - F_{\mathrm{e}\mathrm{K}}(t) - F_{\mathrm{c}\mathrm{K}}(e,t) = 0 \tag{29}$$

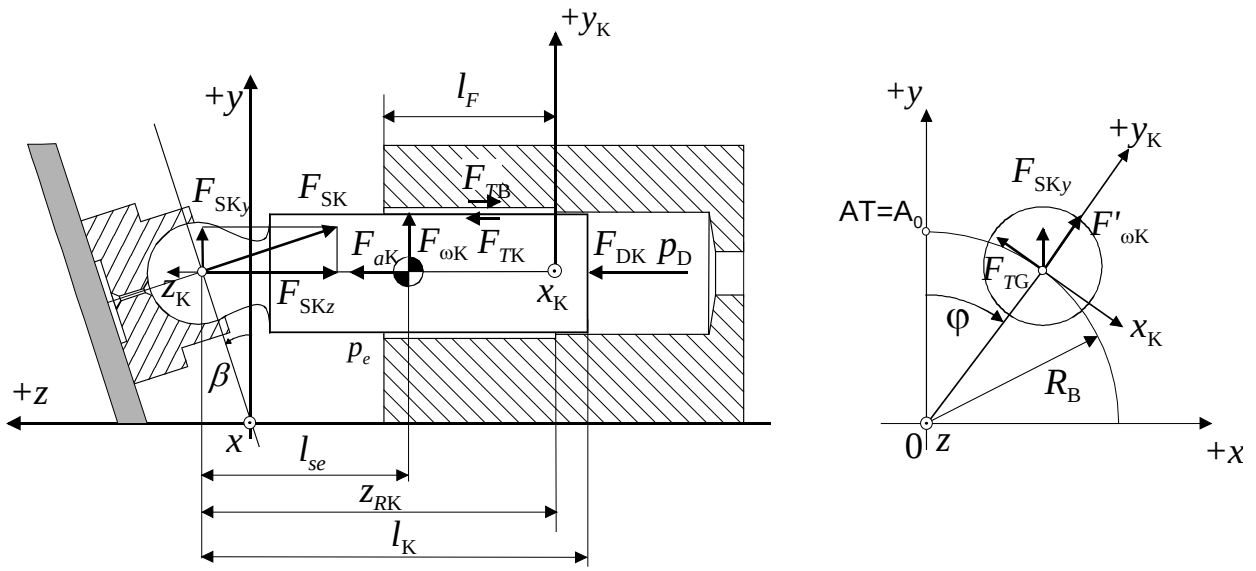

Fig. 7: *External forces applied on the piston*

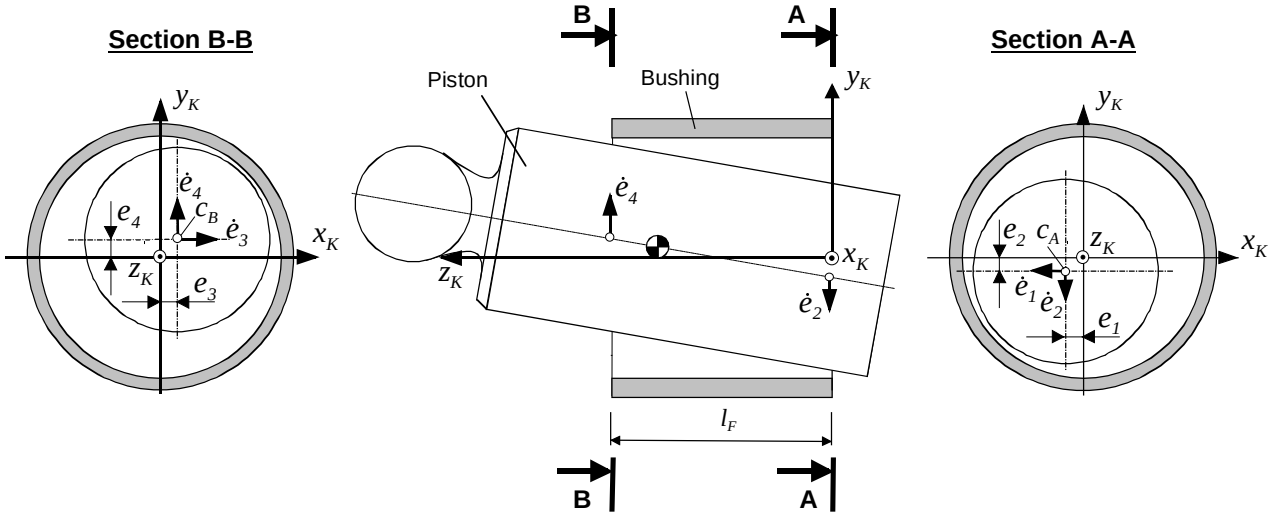

Fig. 8: *Radial movement of the piston*

For a certain shifting velocity of the piston equilibrium of forces can be achieved. Hence Eq. 29 denotes a system of non-linear equations with the shifting velocity as the unknown. To solve this equation the Newton iteration method is used, where **J** denotes the Jacobean of $\mathbf{f_K}$.

$$\dot{\mathbf{e}}^{(m)} = \dot{\mathbf{e}}^{(m-1)} + \frac{1}{2^j}\Delta\dot{\mathbf{e}}^{(m)} \tag{30}$$

$$\Delta\dot{\mathbf{e}}^{(m)} = -\mathbf{J}_K^{-1}(\dot{\mathbf{e}}^{(m-1)})\mathbf{f}_K(\dot{\mathbf{e}}^{(m-1)}) \tag{31}$$

The aim of the evaluation of the motion equation is to modify the position of the components for given external forces, so that with the modified position the system is in an equilibrium state for each considered time step, res. angular position of the cylinder block. The shifting velocity, by which equilibrium of forces is achieved, is obtained by the solution of the motion equation. By integrating the shifting velocity the position of the piston is computed.

Figure 9 shows the calculated radial piston movement during one shaft rotation for the given design and operating parameter. Fig. 9a shows the shifting curve of point c_A on the piston axis in the cross section AA and Fig. 9b the position of point c_B, which is located on the piston axis in cross section BB, see Fig. 8, again over one shaft revolution in eccentricity of the piston. One point on the shifting curve represents the position of the point c_A or c_B respectively at one point of time. For some particular time steps of the simulation the position of c_A and c_B and the associated rotating angles are indicated on the shifting curves. Since c_A and c_B are located opposite to each other at the same rotating angle, the piston is inclined in the cylinder bushing. It can be seen that the eccentricity of point c_B given by e_3 and e_4 (Fig. 9b) increases in the high-pressure stroke for φ = 0° to φ = 180° and decreases in the suction stroke. The eccentricity of point c_A on the piston axis in cross section A-A, is shown in Fig. 9a. When the eccentricity of the piston exceeds the maximum bearing play elastic

deformation of the piston is assumed, so that the clearance between piston and cylinder is not less than a minimum gap height of 0.1 µm, as shown in Fig. 10. Based on the deformation Δw^K and the Young´s modulus the contact force F_{cK} can be calculated. This is a first approach to calculate the flow in case of solid-to-solid contact, since elastohydrodymic effects have not been considered in the simulation model so far.

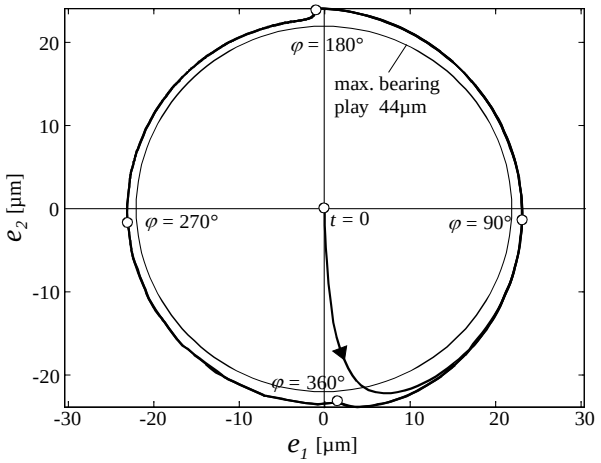

a) Radial movement of the piston in cross section A-A in Fig. 8 - position point c_A

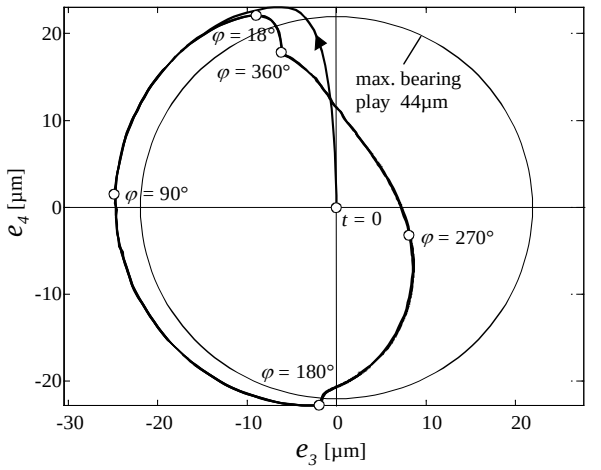

b) Radial movement of the piston in cross section B-B in Fig. 8 - position point c_B

Fig. 9: *Position of the piston*

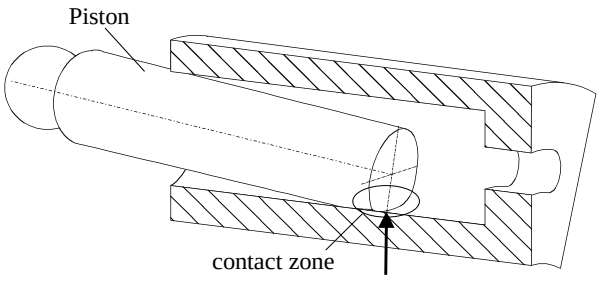

a) inclined piston

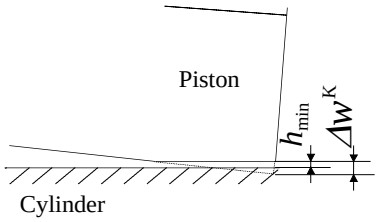

b) Contact zone piston / cylinder

Fig. 10: *Contact force considered for the piston*

6 Simulation Results

6.1 Piston

The gap height and the pressure distribution in the gap for various rotating angles are shown in Fig. 11 and Fig. 12.

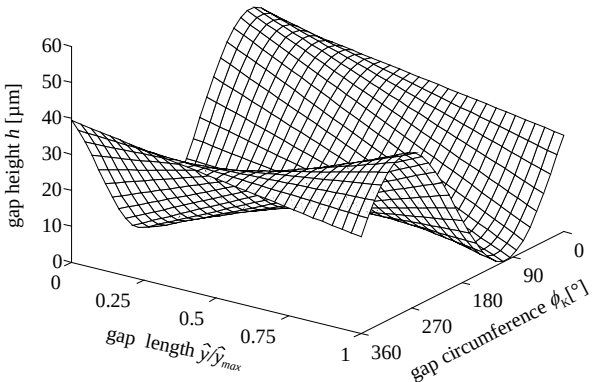

a) $\varphi = 0°$

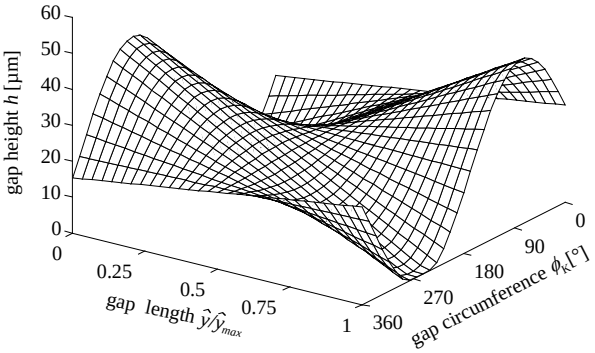

b) $\varphi = 180°$

Fig. 11: *Gap height between piston and cylinder*

The calculated leakage in the gap is shown in Fig. 13. It can be seen that during the high-pressure phase the leakage flow is less than during the low-pressure phase. This can be explained by the fact that under these particular operating conditions the flow due to the piston velocity (Couette-Flow) has the stronger influence than the flow due to the pressure difference (Poiseuille-Flow).

Figure 14 shows the viscous friction force F_{TKy} and F_{TKx} applied on the piston in axial and tangential direction, respectively. In the axial direction the piston velocity mainly influences the friction force. The tangential friction force depends on the relative rotation between piston and cylinder. The rotational speed of the piston is not determined by the kinematics of the assembly. It is determined by the sum of all friction forces acting on the piston (Renius, 1974). Here it is assumed that the piston rotates relative to the cylinder

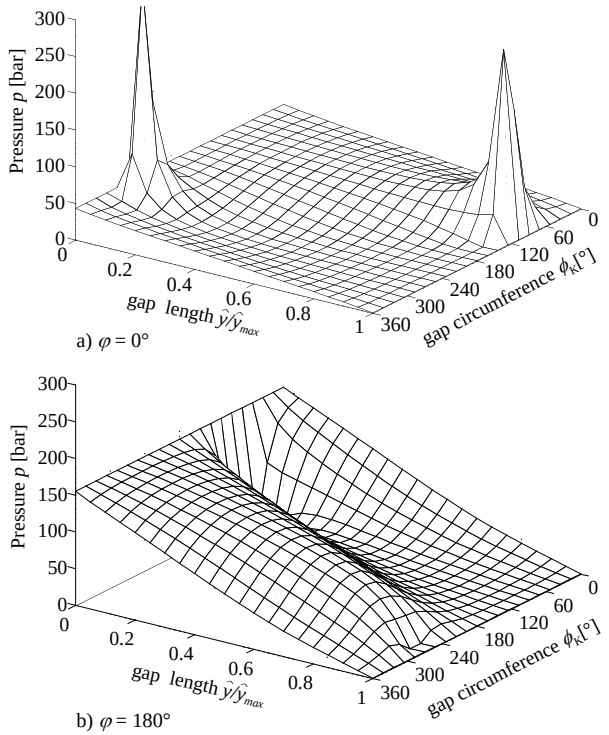

Fig. 12: *Pressure distribution in the gap between piston and cylinder*

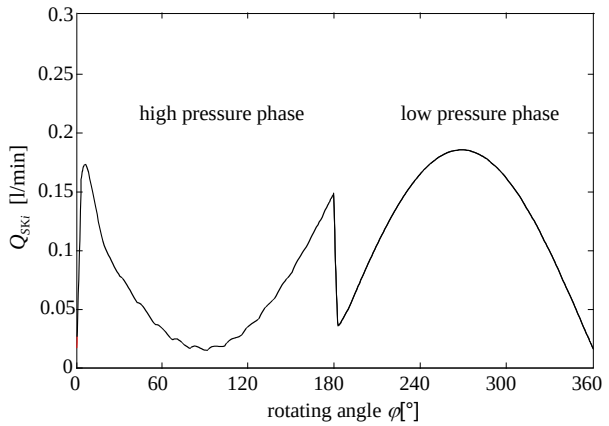

Fig. 13: *Calculated gap flow in the gap between piston and cylinder in axial direction*

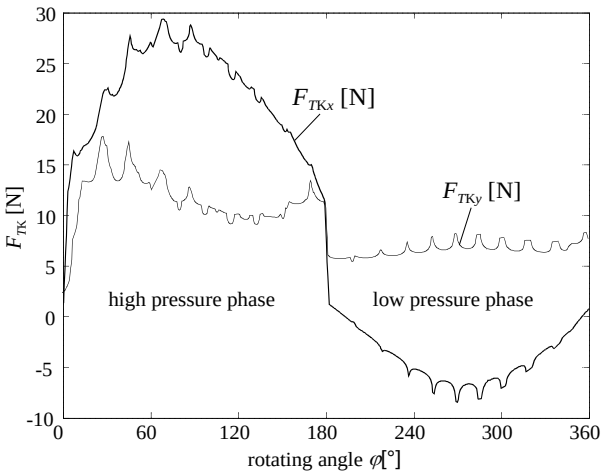

Fig. 14: *Friction forces applied on piston*

block with the rotational speed of the machine. It should been noted that the piston friction forces has been measured with a special test rig under real operating conditions (Lasaar and Ivantysynova, 2001). The comparison between measured piston friction forces and with CASPAR calculated friction force curves has shown a very good fit (Lasaar, 2000).

6.2 Slipper

The position of the slipper can be described by the gap heights between the slipper and swash plate h_{G1}, h_{G2} and h_{G3} in three points, g_1, g_2 and g_3 as shown in Fig. 16. The mathematical model describing the slipper motion as well as the gap flow under the slipper was presented in Wieczorek and Ivantysynova (2000). The calculated gap heights between the slipper and swash plate h_{G1}, h_{G2} and h_{G3} are shown in Fig. 15 for two revolutions. It can be seen that the position converges to a cyclical movement with the same period time as the shaft speed. The simulation starts with the high- pressure phase. It can be seen that, during high-pressure phase, the gap height under the slipper is smaller than in the low-pressure phase due to the larger normal force

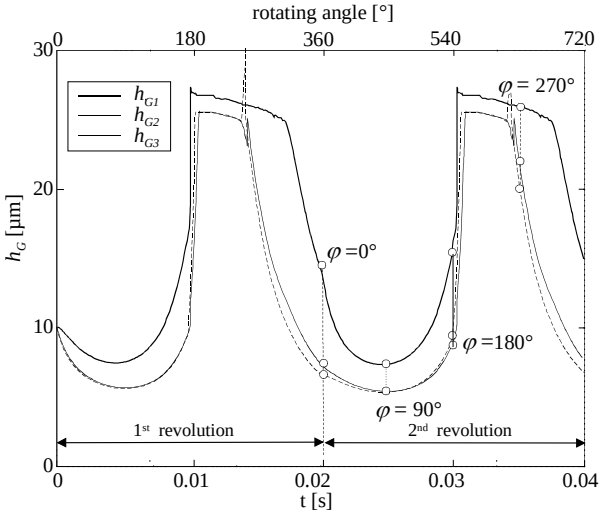

Fig. 15: *Position of the slipper*

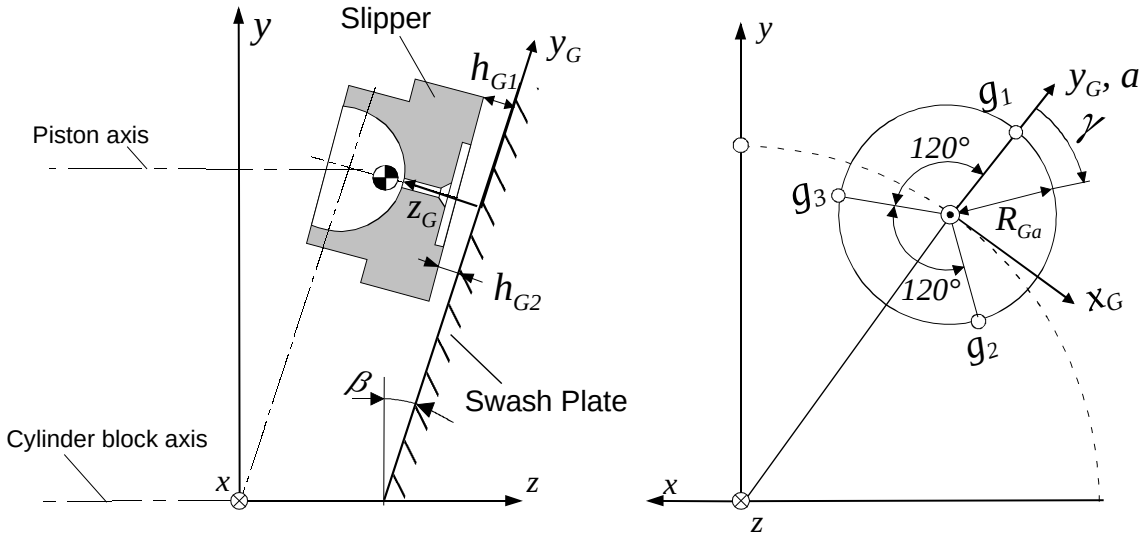

Fig. 16: *Gap height between slipper and swash plate*

applied on the slipper. In the low-pressure phase the retainer prevents the slipper from lifting up. The pressure distribution in the gap are shown in Fig. 18 for φ = 90° and φ = 270°.

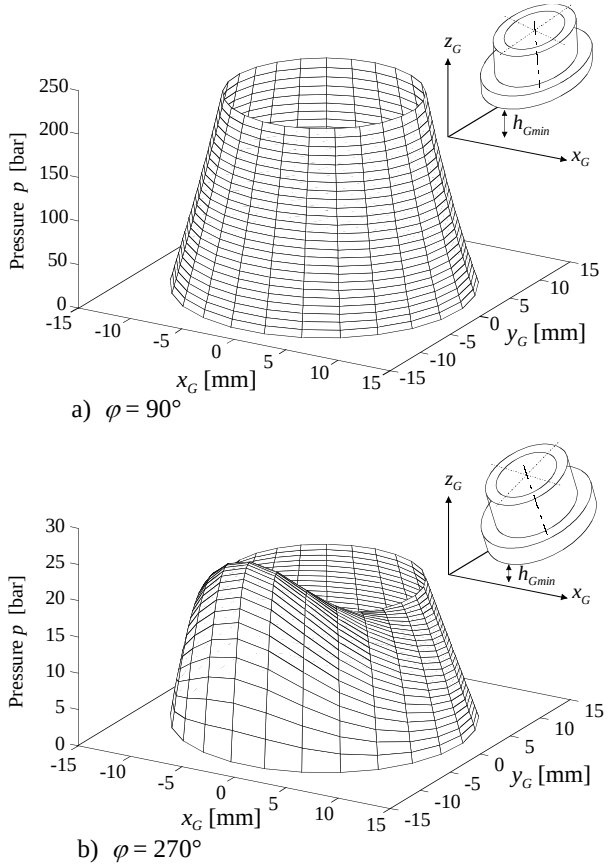

Fig. 17: *Pressure distribution between slipper and swash-plate*

The computed leakage flow under the slipper is shown in Fig. 18. Due to the larger clearance between slipper and swash plate, the leakage flow in low-pressure phases is larger than during high-pressure phases although the pressure is ten times less. The leakage flow of all slippers is obtained by superposition of the 40° phase shifted values of the individual slippers, as shown in Fig. 19. It can be seen that the pulsation of the leakage flow corresponds to the number of pistons, nine peaks occur during one revolution of the pump.

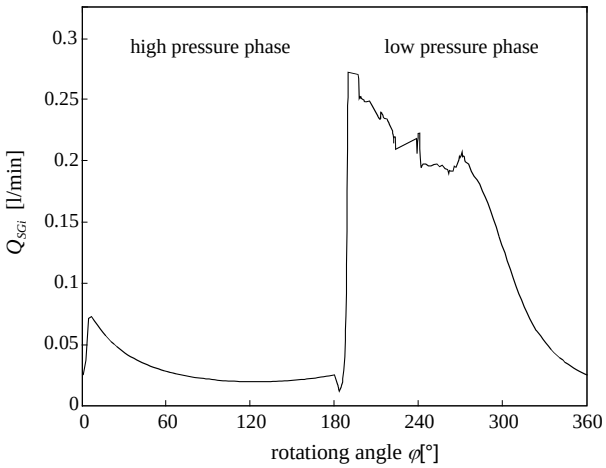

Fig. 18: *Gap flow between one slipper and the swash plate*

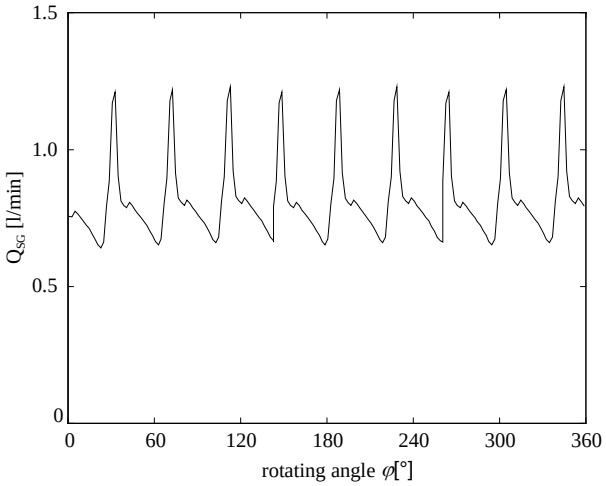

Fig. 19: *Leakage flow of all slippers*

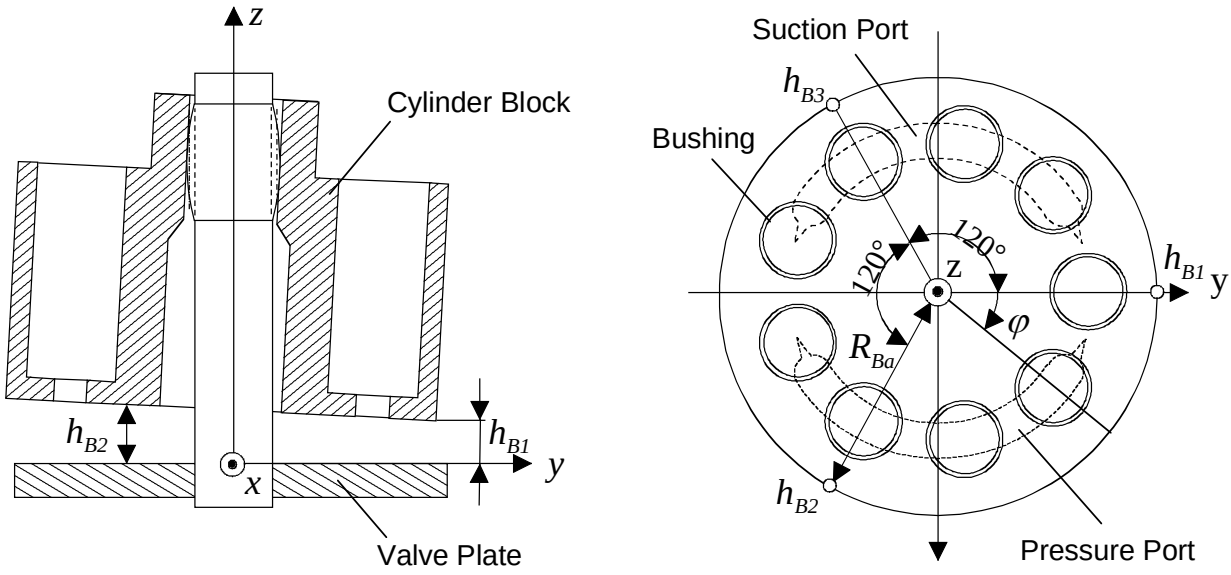

Fig. 20: *Gap height between the cylinder block and the valve plate*

6.3 Cylinder Block

The position of the cylinder block is described by the gap height between cylinder block and valve plate in three points h_{B1}, h_{B2} and h_{B3}, as shown in Fig. 20. The calculation method was presented in Wieczorek (2000). The calculated gap heights h_{B1}, h_{B2} and h_{B3} between cylinder block and valve plate are shown in Fig. 22. The gap heights were simulated over three revolution of the cylinder block. A parallel gap of 2 µm clearance between cylinder block and valve plate is assumed as initial value for the position of the cylinder block.

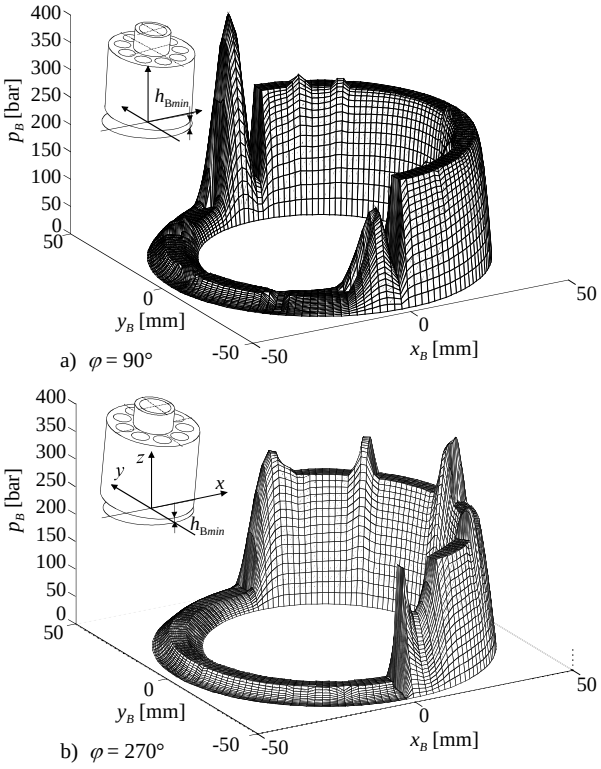

Fig. 21: *Pressure distribution between cylinder block and valve plate*

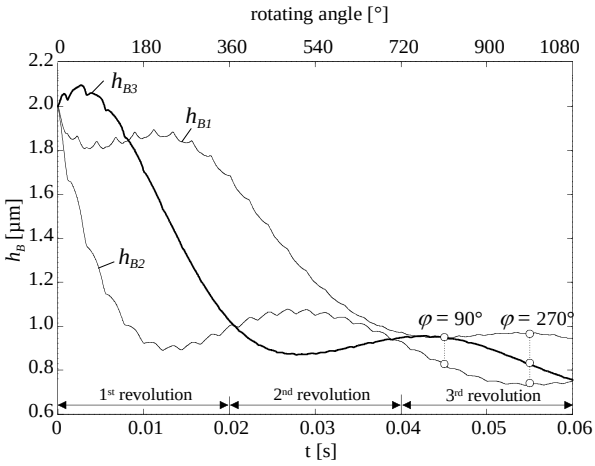

Fig. 22: *Position of the cylinder block*

The pressure distribution in the gap between cylinder block and valve plate obtained from complex gap flow simulation is shown in Fig. 21 for rotating angles of $\varphi = 90°$ and $\varphi = 270°$. The pressure in the pressure port and suction port define the boundary conditions for the pressure field. Due to the fact that high pressure and low pressure are not symmetrically exerted on the cylinder block, the cylinder block is loaded with a tilting moment, which has to be borne by the valve plate. For the leakage flow in the gap between cylinder block and valve plate an average value of Q_{SB} = 0.058 l/min has been calculated. Based on the shearing stress the viscous friction in the gap between cylinder block and valve plate can be calculated. The average torque loss due to viscous friction in the gap between cylinder block and valve plate is M_{SB} = 22.15 Nm for the given example.

6.4 Total Losses

The total external leakage flow Q_{Se} of the displacement machine as shown in Fig. 23, is given by the sum of the gap flows of all pistons Q_{SK}, all slippers Q_{SG} and the gap flow between cylinder block and valve plate Q_{SB}:

$$Q_{Se} = Q_{SK} + Q_{SG} + Q_{SB} \tag{32}$$

For the given example the simulation tool CASPAR computed a total external leakage flow rate of Q_{Se} = 1.70 l/min. During steady state measurements of the in this paper presented swash plate pump an external leakage flow rate of Q_L = 1.68 l/min has been measured under same operating conditions at our test rig. The measurements were performed with a gear flow meter in the pump leakage line. Since the external leakage flow can only be generated in the gaps, which have been considered in the simulation model, the simulation achieves a very good fit here. CASPAR allows further to calculate the instantaneous outlet and inlet flow of the pump. Fig. 24 shows the instantaneous outlet flow for the considered operating parameter of the swash plate pump. The resulting flow ripple is caused by the theoretical non-uniformity of flow, which is given by the pump kinematics, and by the pulsating volumetric losses.

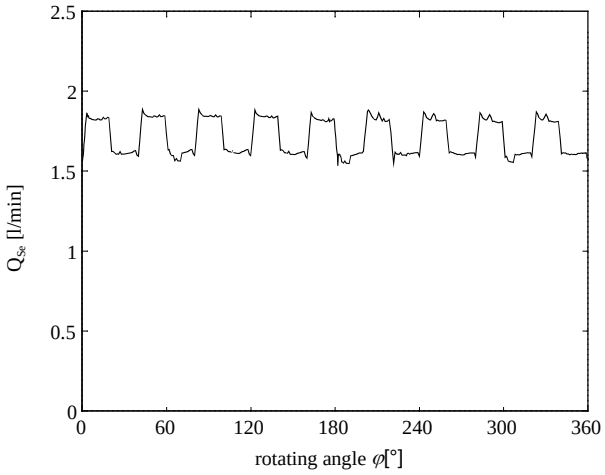

Fig. 23: *Total leakage flow of the swash plate pump - calculated with CASPAR*

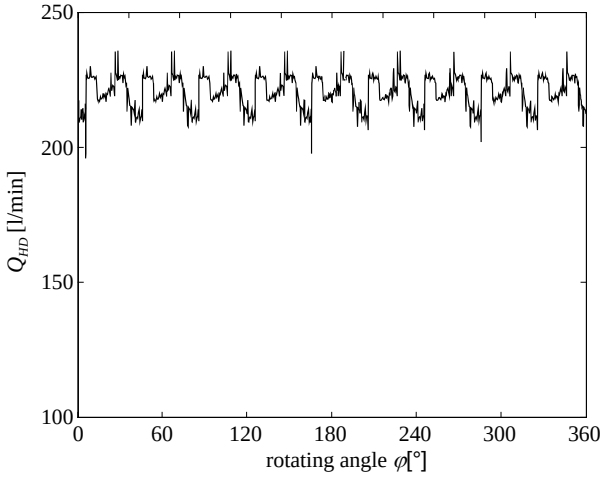

Fig. 24: *Calculated instantaneous pump outlet flow*

The total torque loss due to viscous friction M_S^* is determined by the sum of the torque losses in all gaps:

$$M_S^* = M_{SK} + M_{SG} + M_{SB} \tag{33}$$

For the here considered swash plate pump and the given operating parameter an average torque loss M_S^* of 26.5 Nm was calculated with CASPAR. By using the calculated total leakage flow and the torque loss due to viscous friction forces of all gaps, the total power losses of P_S^* = 8.77 kW have been calculated with CASPAR, Eq. 34 for the given operating parameter of the considered swash plate pump.

$$P_S^* = \omega M_S^* + \Delta p Q_{Se} \tag{34}$$

At the test rig (Ivantysynova 2001) a total power loss of P_S = 10.07 kW have been measured for the same operating point. Due to the fact that not all types of torque losses are considered in CASPAR the calculated losses are always smaller than the measurement results. The churning losses, which are caused by the rotation of the cylinder block in the oil filled case and other torque losses due to friction in roller bearings, are not considered in the simulation model.

6.5 Swash Plate Moment

CASPAR allows also a very precise calculation of the moment exerted on the swash plate due to the piston forces. This is mainly given due to the fact that the simulation model considers all forces exerted on the piston and the slipper including their dependency on the angular position of the cylinder block as well as on the given design and operating parameters. The applied model for calculation of the instantaneous pressure in the displacement chamber considers very precisely the given valve plate design.

To calculate the swash plate moment about the x-axis M_{Sx} the forces that all pistons apply simultaneously on the swash plate have to taken into account for each time step. The swash plate moment is given by:

$$M_{Sx}(\varphi) = \sum_{i=0}^{i=8} F_{N_i}(\varphi + i\,\Delta\varphi)\frac{R_B \cos(\varphi + i\,\Delta\varphi)}{\cos\beta} \tag{35}$$

where i denotes the number of pistons. The swash plate moment obtained from CASPAR is shown in Fig. 26. It can be seen that the swash plate moment changes the sign with a frequency that corresponds to double the number of pistons. The average swash plate moment for the considered operating point is given by 17.98 Nm.

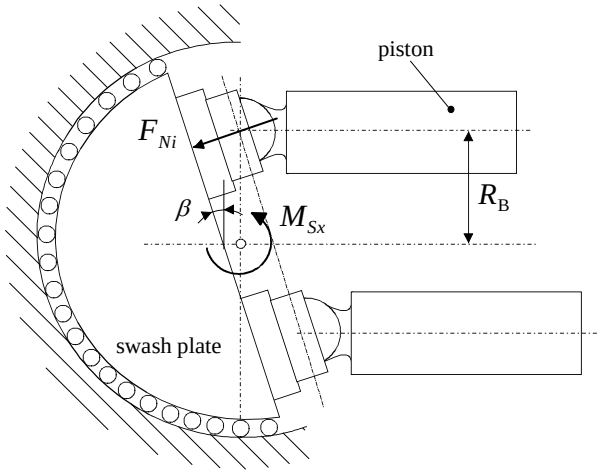

Fig. 25: *Moment exerted on the swash plate due to the piston forces*

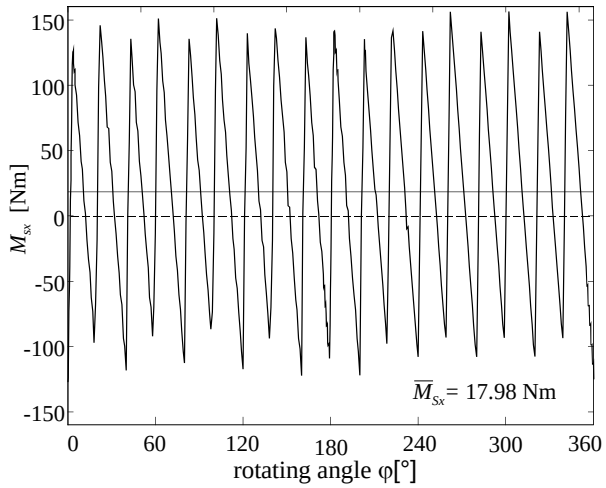

Fig. 26: *Swash plate moment – simulation result*

7 Conclusion

A method for the calculation of the non-isothermal gap flow in the connected gaps of swash plate type axial piston machines has been developed. By solving the motion equation for the moving parts the gap height can be calculated for each considered time step. With the calculated pressure and velocity field, the leakage flow and the viscous friction in the gap can be determined. As mentioned before leakage flow can only occur in the considered gaps, the volumetric losses of a swash plate machine as well as the effective flow rate can be determined precisely in a wide range of operating parameters for different design parameters. The comparison of the simulation data with the measurements, especially the external leakage flow has shown a very good fit. The simulation model only considers viscous friction but this is not a big disadvantage, since viscous friction conditions are the desirable operating conditions of displacement machines. It should be noted that elastohydrodynamic effects are not considered here. In case of solid-to-solid contact a simple approximation is used. Besides this, simulation results for the friction between piston and cylinder were proved by friction measurements on a special test rig (Lasaar and Ivantysynova, 2000). The simulation tool allows the improvement of the efficiency of swash plate machines by optimization of the gap macro geometry without lengthy testing (Lasaar and Ivantysynova, 2002). However in practice a simulation tool cannot replace experiments, it is another approach to support the development.

Nomenclature

c_p	Thermal capacity	[J/kgK]
$\boldsymbol{e}$	Eccentricity of the piston	[m]
$\boldsymbol{f}_K$	Force difference on the piston	[N]
F_{AK}	Axial force applied on piston	[N]
F_{aK}	Inertia force applied on piston	[N]
F_{DK}	Pressure force applied on piston	[N]
$F_{\omega K}$	Centrifugal force applied on piston	[N]
F_{cK}	Contact force applied on piston	[N]
F_{eK}	External force applied on piston	[N]
F_{fK}	Fluid force applied on piston	[N]
F_{SK}	Swash plate reaction force	[N]
F_{TG}	Friction force applied on slipper	[N]
F_{TK}	Friction force applied on piston	[N]
h	Gap height	[m]
$\boldsymbol{h}_G$	Clearance between slipper and swash plate	[m]
$\boldsymbol{h}_B$	Clearance between cylinder block and valve plate	[m]
i	Index piston number	[-]
$\boldsymbol{J}$	Jacobean matrix	[-]
l_F	Bushing length	[m]
M_S^*	Total torque losses (CASPAR Simulation)	[Nm]
M	Torque	[Nm]
M_{fK}	Piston moment due fluid force	[Nm]
M_{Gx}, M_{Gy}	Tilt moment applied on slipper	[Nm]
m_g	Slipper mass	[kg]
m_K	Mass of the piston	[kg]
M_{SK}	Torque losses due to friction on piston	[Nm]
M_{SG}	Torque losses due to friction on slipper	[Nm]
M_{SB}	Torque losses due to friction on cylinder block	[Nm]
M_{Sx}	Swash plate moment	[Nm]
n	Shaft speed	[rpm]
p	Pressure	[Pa]
p_D	Pressure in the displacement chamber	[Pa]
p_e	Case pressure	[Pa]
P_S	Power losses (measurement)	[kW]
P_S^*	Power losses (CASPAR simulation)	[kW]
Q_{HD}	Total flow pressure port	[m³/s]
Q_L	Leakage flow (measurement)	[m³/s]
Q_r	Flow through valve plate	[m³/s]
Q_{SB}	Leakage flow cylinder block	[m³/s]
Q_{Se}	External volumetric losses	[m³/s]
Q_{SG}	Leakage flow slipper	[m³/s]
Q_{SK}	Leakage flow piston	[m³/s]
R_B	Piston pitch radius	[m]
R_{Ga}	Outer radius slipper	[m]
R_K	Radius piston	[m]
Δw^K	Deformation	[m]
t	Time	[sec]
T	Temperature	[K]
V	Displacement chamber volume	[m³]
v_{Kx}, v_{Ky}	Piston velocity in tangential and axial direction	[m/s]
$v_{\hat{x}}, v_{\hat{y}}$	Fluid velocity	[m/s]
$\hat{x}, \hat{y}, \hat{z}$	Co-ordinates gap piston /cylinder	
β	Swash plate angle	[°]
φ	Rotating angle	[rad]
ρ	Density	[kg/m³]
λ	Thermal conductivity	[J/m K]
μ	Viscosity	[Pa s]

τ_{FK}	Wall shear stress	[N/m²]
Φ_D	Dissipation function	[-]
ϕ_K	Angle circumference piston	[rad]
α_P	Pressure coefficient viscosity	[1/Pa]
τ_x, τ_y	Shear stress	[N/m²]
K_T	Temperature coefficient viscosity	[1/K]
x, y, z	Cartesian co-ordinates cylinder block	
x_G, y_G, z_G	Cartesian co-ordinates slipper	
x_K, y_K, z_K	Cartesian co-ordinates piston	
φ, r, z	Cylindrical co-ordinates cylinder block	
γ, a, z_G	Cylindrical co-ordinates slipper	

References

Blackman, L.D. 2001. Detailed Dynamic Model for Variable Displacement Pumps – a new approach with Simulink. *Proc. Recent Advances in Aerospace Actuation Systems and Components*. Toulouse, France, pp. 33-40.

Böninghoff O. 1972. *Das Reibverhalten der Kolben und der Gleitschuhe in Schrägscheiben-Axialkolbenmaschinen*. PhD Thesis, University of Braunschweig, Germany.

Fang Y. and **Shirakashi M.** 1995. Mixed Lubrication Characteristics between the Piston and Cylinder in Hydraulic Piston Pump-Motor. *Journal of Tribology, Trans. ASME*, Vol. 117, pp. 80-85.

Harris, M. R., Edge, K. A. and **Tilley, D. G.** 1993. Predicting the Behaviour of Slipper Pads in Swash-plate-Type Axial Piston Pumps. *ASME Winter Annual Meeting*, New Orleans, Louisiana. 93-WA/FPST-3.

Ivantysyn J. and **Ivantysynova M.** 2001. *Hydrostatic Pumps and Motors*. Academic Books International, New Dehli, India.

Ivantysynova, M. 1999. A New Design to the Design of Sealing and Bearing Gaps of Displacement Machines. *4th JHPS International Symposium on Fluid Power*, Tokyo, Japan.

Ivantysynova, M. 2001. Energy Losses of Modern Displacement Machines- a Approach of Modelling. *7th Scandinavian International Conference on Fluid Power*, Linköping, Sweden, 2001, pp. 377-395.

Ivantysynova M. and **Lasaar R.** 2000. Ein Versuchträger zur Messung der Reibkräfte zwischen Kolben und Zylinder in Axialkolbenmaschinen. *Konstruktion*, Vol. 52, No. 6, pp. 57-65.

Kleist A. 1997. Design of Hydrostatic Static Bearing and Sealing Gaps in Hydraulic Machines. *5th Scandinavian International Conference on Fluid Power*, Lingköping, Sweden.

Krasser J., Laback O., Loinbennegger B. and **Priebsch H.** 1994. Anwendung eines elastohydrodynamischen Verfahrens zur Berechnung von Kurbeltriebslagern. *Motortechnische Zeitschrift*, Vol. 55, pp. 656-663.

Lasaar, R. and **Ivantysynova, M.** 2002. Advanced Gap Design – Basis for Innovative Displacement Machines. *3rd International Fluid Power Conference*, Aachen, Germany, pp. 215-229.

Lasaar, R. 2000. The influence of the Micro and Macro Geometry on the Energy Dissipation in the Lubricating Gaps of Displacement Machines. *Proc. of 1st FPNI PhD Symposium Hamburg 2000***,** pp. 101-116.

Liu, M. 2001. *Dynamisches Verhalten hydrostatischer Axialkolbengetriebe*. PhD thesis. Ruhr-Universität Bochum, Germany.

Olems L. 2000 Investigation of the Temperature Behaviour of the Piston Cylinder Assembly in Axial Piston Pumps. *International Journal of Fluid Power*, Vol. 1 (2000), No. 1, pp. 27-38.

Patankar S. V. 1980. *Numerical Heat Transfer and Fluid Flow*. New York, Washington: Hemisphere Publishing Corporation.

Renius K. T. 1974. *Untersuchungen zur Reibung zwischen Kolben und Zylinder bei Schrägscheiben-Axialkolbenmaschinen*. VDI-Forschungsheft 561. Düsseldorf: VDI-Verlag, Germany.

Sanchen G. 1999 Simulationswerkzeug zur Auslegung von Axialkolbenpumpen in Schrägscheibenbauweise. *O+P Ölhydraulik und Pneumatik*, Vol. 43. Nr. 4, pp. 292-297.

Wieczorek U. and **Ivantysynova M.** 2000. CASPAR – A computer aided design tool for axial piston machines. *Proc. Bath Workshop on Power Transmission and Motion Control PTMC 2000*, Bath, UK, pp. 113-126.

Wieczorek U. 2000. Simulation of the Gap Flow in the Sealing and Bearing Gaps of Axial Piston Machines. *Proc. of 1st FPNI-PhD Symposium Hamburg 2000*, pp. 493-507.

Zhu D., Cheng H. S., Arai T. and **Hamai K.** 1992. A numerical analysis for piston skirt in mixed lubrication. *Journal of Tribology Part I and II*, Vol. 114 and 115, pp. 553-562 and 125-133.

Uwe Wieczorek
Born on June 4th 1968 in Hamburg (Germany) Study of Mechanical Engineering at the TU Hamburg-Harburg. Scientific Employee at the Department of Measurement and Control Engineering of the Gerhard Mercator University of Duisburg. Scientific Employee at the Institute for Aircraft Systems Engineering at the Technical University of Hamburg-Harburg.

Monika Ivantysynova
Born on December 11th 1955 in Polenz (Germany). She received her MSc. Degree in Mechanical Engineering and her PhD. Degree in Hydraulics from the Slovak Technical University of Bratislava, Czechoslovakia. After 7 years in fluid power industry she returned to university. In April 1996 she received a Professorship in fluid power & control at the University of Duisburg (Germany). At present she is Professor of Mechatronic Systems at the Technical University of Hamburg-Harburg. Her research centres around the optimisation of displacement machines, advanced system design and motion control as well as modelling, simulation and testing of fluid power systems. Besides the book “Hydrostatic Pumps and Motors” published in German and English, she has published approximately 45 papers in technical journals and at international conference